OPEN ACCESS
JOURNAL OF ADVANCED DIELECTRICS
Vol. 12, No. 6 (2022) 2241001 (7 pages)

DOI: 10.1142/S2010135X22410016

Influence of the aspect ratio of nitrogen-doped carbon nanotubes on their piezoelectric properties

Marina V. Il'ina*,‡, Olga I. Soboleva†, Nikolay N. Rudyk†, Maria R. Polyvianova†, Soslan A. Khubezhov† and Oleg I. Il'in†

*Southern Federal University, Institute of Nanotechnologies, Electronics and Equipment Engineering
Shevchenko St., 2, Taganrog, 347922, Russia

†Southern Federal University, Research Laboratory of Functional Nanomaterials Technology
Shevchenko St., 2, Taganrog, 347922, Russia

‡mailina@sfedu.ru

Received 26 April 2022; Revised 17 May 2022; Accepted 3 June 2022; Published 7 July 2022

Recent studies have shown that nitrogen doping of carbon nanotubes (CNTs) can lead to the formation of piezoelectric properties in them, not characteristic of pure CNTs. In this work, nitrogen-doped CNTs were grown by plasma-enhanced chemical vapor deposition and the effect of the aspect ratio of the nanotube length to its diameter on its piezoelectric coefficient d_{33} was shown. It was observed that as the aspect ratio of the nanotube increased from 7 to 21, the value of d_{33} increased linearly from 7.3 to 10.7 pm/V. This dependence is presumably due to an increase in curvature-induced polarization because of an increase in the curvature and the number of bamboo-like "bridges" in the nanotube cavity formed as a result of the incorporation of pyrrole-like nitrogen into the nanotube structure. The obtained results can be used in the development of promising elements of nanopiezotronics (nanogenerators, memory elements, and strain sensors).

Keywords: Carbon nanotube; nitrogen; piezoelectric; nanogenerator; PFM.

1. Introduction

Carbon nanotubes (CNTs) are one of the promising materials for modern nanoelectronics and nanosystem technology due to their high conductivity, hardness, elasticity, and scalability.[1–7] In addition, recent studies have shown that the modification of CNTs properties by incorporating nitrogen atoms into the structure of a nanotube opens up new possibilities for their application in making catalysts for lithium-ion batteries, supercapacitors and nanogenerators.[8–12] In this case, the scope of nitrogen-doped CNTs (N-CNTs) depends on the type of nitrogen incorporation into the hexagonal lattice of CNTs. The incorporation of graphite-like nitrogen in N-CNTs leads, on the one hand, to an increase in conductivity due to the formation of a local donor level, and, on the other hand, increases their catalytic activity due to the formation of charged nitrogen centers on the surface. A similar increase in the catalytic activity and surface reactions facilitating the adsorption of reagents is also observed with predominant formation of pyridine-like nitrogen in N-CNTs.[9,13–16] In this case, pyridine-like nitrogen acts as a more active center for reagents desorption and adsorption due to the formation of additional acceptor-like electron state in the form of a vacancy.[9,13,14] As a result, active research on the effect of graphite-like and pyridine-like nitrogen on the electrochemical properties of N-CNTs is carried out to develop efficient catalysts and supercapacitors.[9,17] The formation of pyrrole-like nitrogen in nanotubes leads to the manifestation of anomalous piezoelectric properties of N-CNTs associated with the formation of bamboo-like defects in the nanotube cavity.[12] The bamboo-like defects are graphene sheets formed into the CNT cavity. The formation of such defects is caused by the formation of pentagonal defects in the hexagonal lattice of the nanotube, which lead to the curvature of the graphene sheets into the nanotube and the formation of "bridges". In this case, the value of the piezoelectric strain coefficient of N-CNT can reach up to 200 pm/V,[18] which exceeds the values for the main piezoelectric nanomaterials (ZnO,[19,20] $BaTiO_3$,[21] PVDF[22]) and is comparable with the values for ceramic material based on the PZT system.[23,24] It should be noted that we published our first works on the presence of piezoelectric response in CNTs in 2017.[25,26] Later, it was shown that the value of the piezoelectric coefficient increased with an increase in the defectiveness of CNTs caused by a decrease in the growth temperature.[27] It was only in 2022 when we proposed a mechanism for the occurrence of piezoelectric effect in CNTs that was associated with doping with nitrogen in the pyrrole-like state and the formation of bamboo-like defects.[12] The possibility of efficient conversion of N-CNT nanoscale deformations into a surface potential of up to hundreds of mV and a current of up to hundreds of nA was also shown.[12,28]

‡Corresponding author.

The results obtained suggest that N-CNTs are highly promising for creating nanopiezotronic devices (memory elements, nanogenerators and strain sensors). However, the technological implementation of these devices requires further study of the influence of growth modes of N-CNTs on their piezoelectric properties.

This work is a logical continuation of the abovementioned studies and is aimed at characterizing the piezoelectric response in N-CNTs obtained by plasma-chemical vapor deposition (PECVD) at different heating times of the nickel catalytic film at the stage of catalytic centers formation in order to create promising nanopiezotronic devices based on them.

2. Methods and Materials

2.1. *Growth of N-CNTs*

Nitrogen-doped carbon nanotubes were grown by plasma-enhanced chemical vapor deposition in acetylene (70 sccm) and ammonia (210 sccm) flows acting as carbon and nitrogen precursors, respectively.[29] A silicon wafer was used as a substrate. A TiN film with 100 nm thickness was deposited on the silicon wafer by magnetron sputtering to form the lower electrode. Next, a film of catalytic nickel with thickness of 15 nm was deposited. Then, the Ni/TiN/Si structure was scribbled into 5×5 mm^2 substrates and placed in a PECVD chamber, where heating was carried out to 660°C for 14, 16 and 18 min in argon (40 sccm) and ammonia (15 sccm) flows. As a result, Ni catalytic centers were formed for the subsequent growth of vertically aligned N-CNTs.[30] The growth time was 15 min. And, the plasma power was 43 W (430 V, 0.1 A).

2.2. *Characterization of N-CNTs*

Geometric parameters of the N-CNTs were defined with the help of scanning electron microscopy (SEM) using Nova NanoLab 600 (FEI, Netherlands). The surface composition and chemical state of the N-CNTs were determined by X-ray photoelectron spectroscopy (XPS) using the K-Alpha ThermoScientific equipment with a monochromatic X-ray source Al Kα (hν = 1486.6 eV). The structural analysis of the N-CNTs was conducted by the transmission electron microscopy (TEM) using Tecnai Osiris (FEI, Netherlands).

The study of the piezoelectric properties of the N-CNTs was performed by piezoresponse force microscopy (PFM) in jumping (or hybrid) mode. The piezoresponse distribution map was built on the basis of a set of force curves when an alternating voltage (1 V, 5 kHz) was applied at the moment the probe touched the sample. We used HA_NC probe with a conductive Pt coating with a force constant of 12 N/m, a resonant frequency of 235 kHz and a tip diameter of 20 nm. Jumping mode of the PFM is a more sparing research technique and does not lead to the separation of vertically aligned N-CNTs from the substrate during scanning, similar to how it is observed for contact methods of atomic force microscopy.[31] The piezoelectric strain coefficient d_{33} of N-CNTs was determined on the basis of the dependence of the mechanical vibration amplitude of the nanotube on the value of the alternating voltage pulse $U = U_{DC} + U_{AC}(\sin(\varphi t))$ with U_{DC} of ± 8 V, U_{AC} of ± 1.0 V and φ of 5 kHz. The magnitude of the piezoelectric strain coefficient N-CNTs was determined as $d_{33} = k \cdot dA/dU_{DC}$,[32] where A is the displacement amplitude of the AFM probe under the action of the applied voltage, k is the proportionality factor that determines the that relates the measured vibration amplitude in nA to the surface displacement in pm. The proportionality factor k was pre-calibrated for this PFM measurement system and is equal to 18.81 pm/nA.

3. Results and Discussion

Analysis of SEM images of N-CNTs experimental samples showed that the heating time of the nickel catalytic layer influenced the geometric parameters of nanotubes (Fig. 1).

Thus, with an increase in heating time from 14 to 18 min, the diameter of N-CNTs decreased from 106 ± 26 to 59 ± 18 nm, and the length increased from 830 ± 102 to 1254 ± 95 nm (Fig. 1). In this case, a decrease in the diameter of nanotubes led to a corresponding increase in the density of nanotubes in an array from 12 to 28 μm^{-2}. This pattern is probably associated with an increase in the heating rate and, as a result, with an increase in the rate of surface diffusion of nickel during heating of the Ni film, which led to the coagulation of small catalytic centers into larger centers and an increase in the uniformity of their distribution over diameters with a decrease in heating time. A change in the diameter of the formed catalytic centers, in turn, led to a subsequent change in the diameter of N-CNTs. The effect of temperature and heating time on the formation of catalytic centers was described in detail in Ref. 30.

Analysis of the XPS spectra showed that the experimental samples had similar chemical composition and contained 57 atomic percent (at.%) of carbon, 19 at.% of oxygen, 11.4 at. % of nitrogen, 10.6 at.% of titanium and 2 at.% of nickel. The high nitrogen concentration is due to the influence of the signal detected from the TiN sublayer. At the same time, the analysis of the high-resolution spectra of Ti2p and N1s showed that about 8% of nitrogen was in the TiN sublayer, the remaining 3.4% of nitrogen was incorporated into the nanotube structure. The analysis of the high-resolution spectrum C1s showed (Fig. 2(a)) that there were energy peaks for the C=C bond (284.6 eV) characteristic of sp_2 hybridization of carbon and for the C–C bond (284.8 eV) caused by the presence of adsorbed adventitious carbon and defects in the two-dimensional structure of the graphene sheet. A significant amount of bonds (about 18 at.%) of carbon with nitrogen, which are characteristic of nitrogen-doped CNTs, were also detected. The presence of an adsorption layer of atmospheric oxygen on the surface of N-CNTs led to

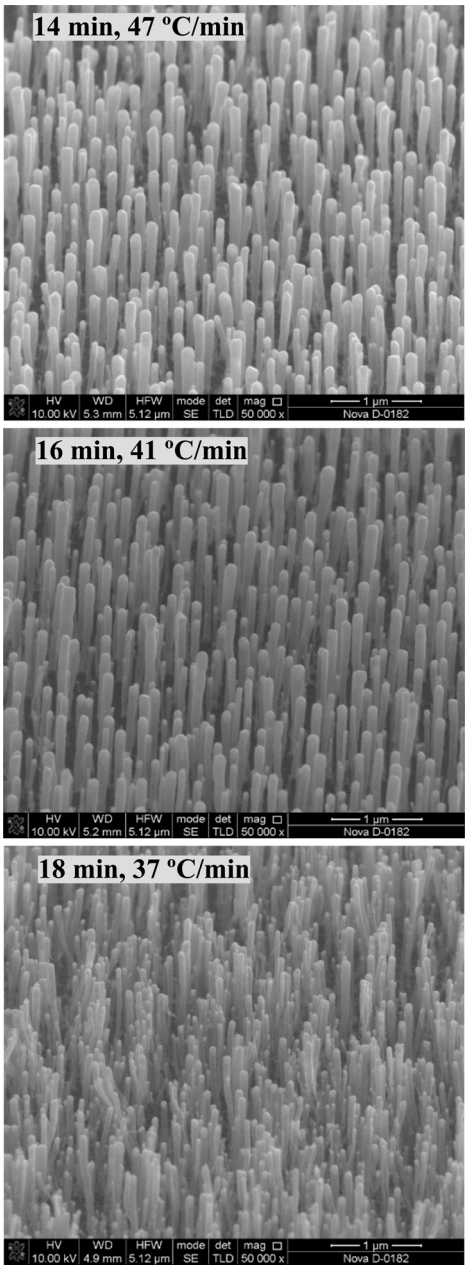

Fig. 1. SEM images of N-CNTs arrays grown on a Ni/TiN/Si structure subjected to different heating times at the stage of catalytic centers formation.

the formation of C–O (286.1 eV) and C=O (288.5 eV) bonds with oxygen (about 10%). An energy peak (283.6 eV) was also observed, corresponding to nonstoichiometric nickel carbide (about 3 at.%), which was formed during the growth of N-CNTs on the surface of the catalytic Ni particle.

The high-resolution spectrum N1s showed that there were intensity peaks associated with signal detection from the TiN sublayer and its oxide (397.5 and 396.5 eV, respectively) and intensity peaks associated with nanotube doping (Fig. 2(b)). An analysis of the peaks corresponding to the incorporation of nitrogen into the nanotube structure showed that nitrogen was predominantly (35%) in the pyridine-like form (398.5–398.8 eV[13,16,33]), which led to the formation of vacancies in the hexagonal lattice of the nanotube. The oxidized form of pyridine-like nitrogen (403.2 eV) was also present, the concentration of which was 14%. The concentration of graphite-like nitrogen (401.1 eV[13,16,33]), which replaced carbon atoms at the sites of the CNT hexagonal lattice, was 23%. The concentration of nitrogen in the pyrrole-like form (400.1–400.2 eV[13,16,33]), which corresponded to the substitution of carbon atoms at lattice site with the formation of pentagonal defects and led to the formation of bamboo-like structural defects,[15,34,35] was 15%. The process of incorporation of the pyrrole-like nitrogen with the formation of a pentagonal defect competes with the incorporation of the graphitic-like or pyridine-like nitrogen with the formation of a regular hexagon due to different rates of surface diffusion of new carbon and nitrogen atoms to the "catalyst-graphene sheet" growth boundary of the nanotube.[12–15] The formation of pentagon defects is observed when the flux of surface diffusion of carbon atoms decreases and the characteristic time of arrival of a new carbon atom at the growth boundary becomes longer than the characteristic time of formation of a pentagon defect.[35] This process can be controlled by changing the growth temperature and the ratio of process gas flows of acetylene and ammonia.[12–14] The mechanism of the formation of bamboo-like defects in CNTs is described in more detail in Refs. 15, 34 and 35.

PFM studies of the samples showed that a significant vertical piezoresponse was detected at the tops of the N-CNTs (Figs. 3(a)–3(c)). Analysis of the vertical piezoresponse phase signal (Fig. 3(d)) suggests the direction of polarization along N-CNTs: the polarization vector is directed from the top to the base of the nanotube. The magnitude of the lateral piezoresponse of N-CNTs was 5–6 times less than the vertical piezoresponse (Fig. 3(d)), with the predominant direction of the longitudinal polarization vector from the center to the side surface of the nanotube. The analysis of PFM images allows us to speak about the predominant direction of polarization along the nanotube axis.

To quantify the vertical piezoresponse of N-CNTs, piezoelectric strain coefficient d_{33} values were calculated for all samples (Fig. 4). It was found that the value of d_{33} increased from 7.3 ± 0.2 to 10.7 ± 0.9 pm/V with an increase in the heating time of the Ni/TiN/Si structure from 14 to 18 min (Table 1). The calculated values of d_{33} were lower than in Refs. 12 and 18, which was associated with a lower concentration of pyrrole nitrogen.

The dependence of the piezoelectric strain coefficient of N-CNTs on the heating time of the Ni/TiN/Si structure is probably due to a change in the diameter and length of the nanotubes as a result of a change in the geometric parameters of the Ni catalytic centers (Table 1). Thus, we previously established that the occurrence of the piezoelectric effect in carbon nanotubes is due to the incorporation of pyrrole-like

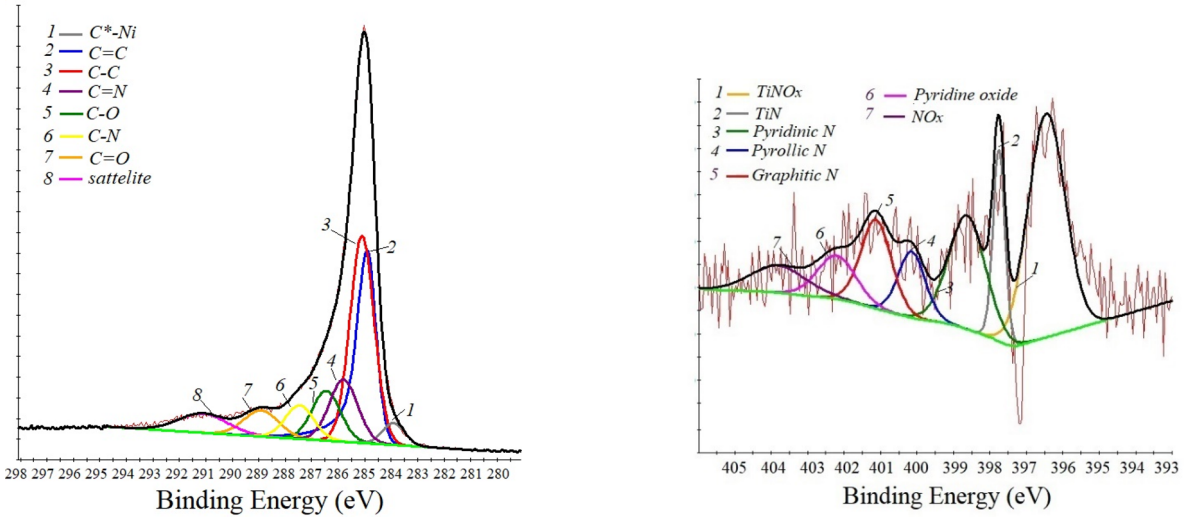

Fig. 2. High-resolution XPS spectrum C1s (a) and N1s (b) of the N-CNTs grown on a Ni/TiN/Si structure after 14 min of heating.

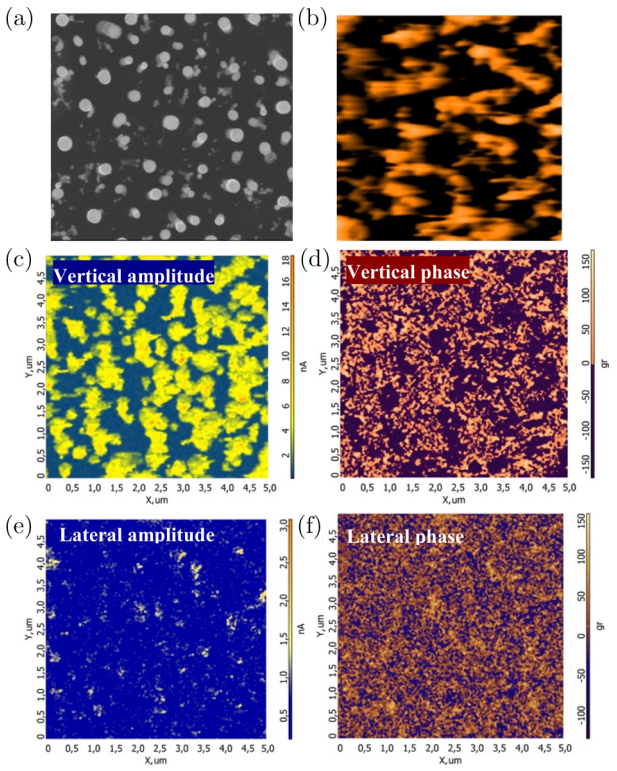

Fig. 3. (a) SEM image (top view) with size 5×5 μm^2 and PFM study: (b) Topography image with size 5×5 μm^2, (c, d) vertical piezoelectric response and (e, f) lateral piezoelectric response of the N-CNTs grown on an Ni/TiN/Si structure after 14 min of heating.

nitrogen into their structure, which leads to the formation of bamboo-like defects.[12] In turn, bamboo-like defects are the source of curvature-induced polarization[36] caused by the curvature of the graphene sheet, which forms a characteristic "bridge" in the cavity of N-CNTs (Fig. 5).

As a result, an increase in the diameter of N-CNTs leads to a decrease in the curvature of the graphene sheet surface, which forms a bamboo-like "bridge", thus causing a decrease in the electric dipole moment $\boldsymbol{p}_i$.[37] Hence, the piezoelectric strain coefficient of N-CNTs decreases with an increase in a nanotube diameter (Table 1). On the other hand, the total value of curvature-induced polarization $\boldsymbol{P}$ is the ratio of the sum of $\boldsymbol{p}_i$ formed by each bamboo-like "bridge" of a vertically aligned nanotube to its volume (Fig. 5). This fact leads to an increase in the piezoelectric strain coefficient of N-CNTs with an increase in its length, since the sum of the dipole moments increases significantly. To simultaneously consider these dependencies, it is convenient to use such a characteristic of carbon nanotubes as the aspect ratio of their length to diameter. The dependence of the piezoelectric strain coefficient of the N-CNTs on the aspect ratio is shown in Fig. 4(b). It can be seen that with an increase in the aspect ratio of N-CNTs, the value of d_{33} increases linearly. At the same time, it should be noted that an increase in the density of N-CNTs in an array with a decrease in their diameter does not affect the value of the d_{33}. However, there may be an increase in the piezoelectric response, which is the current detected during the nanotube deformation, with an increase in the N-CNT density in the array.[12] This fact is due to an increase in the number of N-CNTs in contact with the probe during the measurement. The obtained pattern is in good agreement with the previously proposed mechanism for the occurrence of piezoelectric effect in nitrogen-doped carbon nanotubes[12] and fundamental theory of nanopiezotronics.[38]

Thus, the aspect ratio of N-CNTs is a significant factor influencing their piezoelectric response under the condition of an equal concentration of nitrogen defects. At the same time, it should be noted that it is the value of the concentration of nitrogen defects, primarily pyrrole-like nitrogen, that

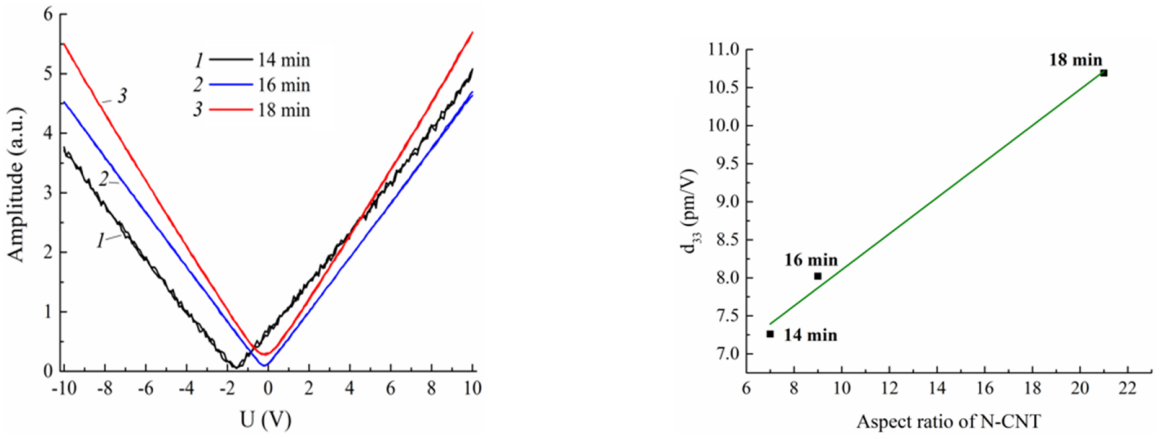

(a) (b)

Fig. 4. PFM amplitude of the vertical piezoelectric response on the amplitude of the applied voltage to the probe (a) and the dependence of the piezoelectric strain coefficient on the aspect ratio of N-CNTs; (b) points show experimental values and solid line denotes approximating dependence.

Table 1. Characterization of N-CNTs grown on an Ni/TiN/Si structure after heating at different duration.

Heating time, min	Diameter, nm	Length, nm	Aspect ratio	d_{33}, pm/V
14	106 ± 26	831 ± 102	7	7.3 ± 0.2
16	104 ± 22	917 ± 90	9	8.5 ± 0.6
18	59 ± 18	1254 ± 95	21	10.7 ± 0.9

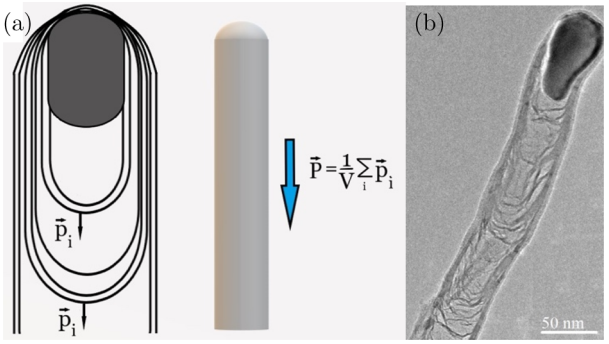

Fig. 5. Schematic representation of bamboo-like defects in N-CNTs associated with the curvature of the graphene polarization plane P (a) and TEM image of the N-CNT (b). Polarization is the ratio of the sum of electric dipole moments p_i formed by each bamboo-like "bridge" to the volume V of the nanotube.

is the main factor determining the value of the piezoelectric strain coefficient of N-CNTs.[12]

4. Conclusion

Thus, we have shown that the piezoelectric strain coefficient of the N-CNTs increases linearly with the aspect ratio of their length to diameter. In this case, the value of the aspect ratio of N-CNTs depends on the heating rate of the nickel catalytic film at the stage of catalytic centers formation. A change in the heating rate makes it possible to vary the diameter of catalytic centers, which subsequently determines the geometric parameters of nanotubes. At the same time, a change in the heating rate does not lead to a change in the concentration and type of nitrogen defects in N-CNTs. The results obtained make it possible to control the magnitude of the piezoelectric response of N-CNTs for a given amount of nitrogen doping. The established pattern can be used in the development of promising elements of nanopiezotronics, including energy-efficient nanogenerators and memory elements.

Acknowledgments

This study was financially supported by the Ministry of Science and Higher Education of the Russian Federation; the state task in the field of scientific activity No. FENW-2022-0001.

References

[1]B. Liu, C. Wang, J. Liu, Y. Che and C. Zhou, Aligned carbon nanotubes: From controlled synthesis to electronic applications, *Nanoscale* **5**, 9483 (2013), https://doi.org/10.1039/c3nr02595k.
[2]K. Matsumoto, *Frontiers of Graphene and Carbon Nanotubes* (Springer Japan, Tokyo, 2015), https://doi.org/10.1007/978-4-431-55372-4.
[3]A. D. Franklin, Carbon nanotube electronics, in *Emerg. Nanoelectron. Devices* (John Wiley & Sons Ltd, Chichester, United Kingdom, 2014), pp. 315–335. https://doi.org/10.1002/9781118958254.ch16.
[4]C. H. Ke, N. Pugno, B. Peng and H. D. Espinosa, Experiments and modeling of carbon nanotube-based NEMS devices, *J. Mech. Phys. Solids*. **53**, 1314 (2005), https://doi.org/10.1016/j.jmps.2005.01.007.
[5]L. Wang, C. Yang, J. Wen, S. Gai and Y. Peng, Carbon nanotubes: Synthesis and properties, electronic devices and other emerging applications, *J. Mater. Sci. Mater. Electron.* **26**, 4618 (2015), https://doi.org/10.1179/174328004X5655.

[6]S. Abdalla, F. Al-Marzouki, A. A. Al-Ghamdi and A. Abdel-Daiem, Different technical applications of carbon nanotubes, *Nanoscale Res. Lett.* **10**, 358 (2015), https://doi.org/10.1186/s11671-015-1056-3.

[7]M. M. Altarawneh, G. A. Alharazneh and O. Y. Al-Madanat, Dielectric properties of single wall carbon nanotubes-based gelatin phantoms, *J. Adv. Dielectr.* **8**, 1 (2018), https://doi.org/10.1142/S2010135X18500108.

[8]W. J. Lee, U. N. Maiti, J. M. Lee, J. Lim, T. H. Han and S. O. Kim, Nitrogen-doped carbon nanotubes and graphene composite structures for energy and catalytic applications, *Chem. Commun.* **50**, 6818 (2014), https://doi.org/10.1039/c4cc00146j.

[9]S. N. Faisal, E. Haque, N. Noorbehesht, W. Zhang, A. T. Harris, T. L. Church and A. I. Minett, Pyridinic and graphitic nitrogen-rich graphene for high-performance supercapacitors and metal-free bifunctional electrocatalysts for ORR and OER, *RSC Adv.* **7**, 1(2017), https://doi.org/10.1039/c7ra01355h.

[10]C. Cao, Y. Zhou, S. Ubnoske, J. Zang, Y. Cao, P. Henry, C. B. Parker and J. T. Glass, Highly stretchable supercapacitors via crumpled vertically aligned carbon nanotube forests, *Adv. Energy Mater.* **9**, 1 (2019), https://doi.org/10.1002/aenm.201900618.

[11]X. Zhang, Z. Zhao, J. Xu, Q. Ouyang, C. Zhu, X. Zhang, X. Zhang and Y. Chen, N-doped carbon nanotube arrays on reduced graphene oxide as multifunctional materials for energy devices and absorption of electromagnetic wave, *Carbon* **177**, 216 (2021), https://doi.org/10.1016/j.carbon.2021.02.085.

[12]M. Il'ina, O. Il'in, O. Osotova, S. Khubezhov, N. Rudyk, I. Pankov, A. Fedotov and O. Ageev, Pyrrole-like defects as origin of piezoelectric effect in nitrogen-doped carbon nanotubes, *Carbon* **190**, 348 (2022), https://doi.org/10.1016/j.carbon.2022.01.014.

[13]M. Inagaki, M. Toyoda, Y. Soneda and T. Morishita, Nitrogen-doped carbon materials, *Carbon* **132**, 104 (2018), https://doi.org/10.1016/j.carbon.2018.02.024.

[14]L.G. Bulusheva, A. V. Okotrub, Y. V. Fedoseeva, A.G. Kurenya, I. P. Asanov, O. Y. Vilkov, A. A. Koós and N. Grobert, Controlling pyridinic, pyrrolic, graphitic, and molecular nitrogen in multi-wall carbon nanotubes using precursors with different N/C ratios in aerosol assisted chemical vapor deposition, *Phys. Chem. Chem. Phys.* **17**, 23741 (2015), https://doi.org/10.1039/c5cp01981h.

[15]B. G. Sumpter, V. Meunier, J.M. Romo-Herrera, E. Cruz-Silva, D. A. Cullen, H. Terrones, D. J. Smith and M. Terrones, Nitrogen-mediated carbon nanotube growth: Diameter reduction, metallicity, bundle dispersability, and bamboo-like structure formation, *ACS Nano* **1**, 369 (2007), https://doi.org/10.1021/nn700143q.

[16]R. Arenal, K. March, C. P. Ewels, X. Rocquefelte, M. Kociak, A. Loiseau and O. Stéphan, Atomic configuration of nitrogen-doped single-walled carbon nanotubes, *Nano Lett.* **14**, 5509 (2014), https://doi.org/10.1021/nl501645g.

[17]O. Y. Podyacheva, S. V. Cherepanova, A. I. Romanenko, L. S. Kibis, D. A. Svintsitskiy, A. I. Boronin, O. A. Stonkus, A. N. Suboch, A. V. Puzynin and Z. R. Ismagilov, Nitrogen doped carbon nanotubes and nanofibers: Composition, structure, electrical conductivity and capacity properties, *Carbon* **122**, 475 (2017), https://doi.org/10.1016/j.carbon.2017.06.094.

[18]M. V. Il'ina, O. I. Il'in, A. V. Guryanov, O. I. Osotova, Y. F. Blinov, A. A. Fedotov and O. A. Ageev, Anomalous piezoelectricity and conductivity in aligned carbon nanotubes, *J. Mater. Chem. C* **9**, 6014 (2021), https://doi.org/10.1039/d1tc00356a.

[19]L. Wang, S. Liu, G. Gao, Y. Pang, X. Yin, X. Feng, L. Zhu, Y. Bai, L. Chen, T. Xiao, X. Wang, Y. Qin and Z. L. Wang, Ultrathin piezotronic transistors with 2 nm channel lengths, *ACS Nano* **12**, 4903 (2018), https://doi.org/10.1021/acsnano.8b01957.

[20]Y. Hu and Z. L. Wang, Recent progress in piezoelectric nanogenerators as a sustainable power source in self-powered systems and active sensors, *Nano Energy* **14**, 3 (2014), https://doi.org/10.1016/j.nanoen.2014.11.038.

[21]I. Choi, S. J. Lee, J. C. Kim, Y. Gyu Kim, D. Y. Hyeon, K. S. Hong, J. Suh, D. Shin, H. Y. Jeong and K. Il Park, Piezoelectricity of picosecond laser-synthesized perovskite $BaTiO_3$ nanoparticles, *Appl. Surf. Sci.* **511**, 145614 (2020), https://doi.org/10.1016/j.apsusc.2020.145614.

[22]P. Viswanath, K. K. H. De Silva, H. H. Huang and M. Yoshimura, Large piezoresponse in ultrathin organic ferroelectric nano lamellae through self-assembly processing, *Appl. Surf. Sci.* **532**, 147188 (2020), https://doi.org/10.1016/j.apsusc.2020.147188.

[23]I. Andryushina, A. Pavlenko, S. Zinchenko, K. Andryushin, L. Shilkina, E. Glazunova, A. Nagaenko, D. Stryukov, H. Sadykov and L. Reznichenko, Obtaining, structure, microstructure and dielectric characteristics of ceramics and thin films of ferro-piezoelectric materials based on the PZT system, *J. Adv. Dielectr.* **10**, 1 (2020), https://doi.org/10.1142/S2010135X20600036.

[24]N. Kunnath and J. Philip, Dielectric and piezoelectric perfomance of lead-free ceramics of boron sodium gadolinate niobate at morphotropic phase boundary, *J. Adv. Dielectr.* **10**, 1 (2020), https://doi.org/10.1142/S2010135X20500149.

[25]M. V. Il'ina, O. I. Il'in, Y. F. Blinov, V. A. Smirnov, A. S. Kolomiytsev, A. A. Fedotov, B. G. Konoplev and O. A. Ageev, Memristive switching mechanism of vertically aligned carbon nanotubes, *Carbon* **123**, 514 (2017), https://doi.org/10.1016/j.carbon.2017.07.090.

[26]M. V. Ilina, Y. F. Blinov, O. I. Ilin, N. N. Rudyk and O. A. Ageev, Piezoelectric effect in non-uniform strained carbon nanotubes, *IOP Conf. Ser. Mater. Sci. Eng.* **256**, 012024 (2017), https://doi.org/10.1088/1757-899X/256/1/012024.

[27]M. V. Il'ina, O. I. Il'in, N. N. Rudyk, O. I. Osotova, A. A. Fedotov and O. A. Ageev, Analysis of the piezoelectric properties of aligned multi-walled carbon nanotubes, *Nanomaterials* **11**, 2912 (2021), https://doi.org/10.3390/nano11112912.

[28]M. Il'ina, O. Il'in, Y. Blinov, A. Konshin, B. Konoplev and O. Ageev, Piezoelectric response of multi-walled carbon nanotubes, *Materials* **11**, 638 (2018), https://doi.org/10.3390/ma11040638.

[29]O. I. Il'in, M. V. Il'ina, N. N. Rudyk, A. A. Fedotov and O. A. Ageev, Vertically aligned carbon nanotubes production by PECVD, in *Perspect. Carbon Nanotub.* (IntechOpen, 2019), p. 13, https://doi.org/10.5772/intechopen.84732.

[30]O. Il'in, N. Rudyk, A. Fedotov, M. Il'ina, D. Cherednichenko and O. Ageev, Modeling of catalytic centers formation processes during annealing of multilayer nanosized metal films for carbon nanotubes growth, *Nanomaterials* **10**, 554 (2020), https://doi.org/10.3390/nano10030554.

[31]M. V. Il'ina, O. I. Il'in, V. A. Smirnov, Y. F. Blinov, B. G. Konoplev and O. A. Ageev, Scanning probe techniques for characterization of vertically aligned carbon nanotubes, in *At. Microsc. Its Appl.* (IntechOpen, 2019), p. 13, https://doi.org/10.5772/intechopen.78061.

[32]S. M. Neumayer, S. Saremi, L. W. Martin, L. Collins, A. Tselev, S. Jesse, S. V. Kalinin and N. Balke, Piezoresponse amplitude and phase quantified for electromechanical characterization, *J. Appl. Phys.* **128**, 171105 (2020), https://doi.org/10.1063/5.0011631.

[33]Y. Yamada, J. Kim, S. Matsuo and S. Sato, Nitrogen-containing graphene analyzed by X-ray photoelectron spectroscopy, *Carbon* **70**, 59 (2014), https://doi.org/10.1016/j.carbon.2013.12.061.

[34]M. Lin, J. P. Y. Tan, C. Boothroyd, K. P. Loh, E. S. Tok and Y. L. Foo, Dynamical observation of bamboo-like carbon nanotube growth, *Nano Lett.* **7**, 2234 (2007), https://doi.org/10.1021/nl070681x.

[35]O. A. Louchev, Formation mechanism of pentagonal defects and bamboo-like structures in carbon nanotube growth mediated by surface diffusion, *Phys. Status Solidi Appl. Res.* **193**, 585 (2002), https://doi.org/10.1002/1521-396X(200210)193:3<585::AID-PSSA585>3.0.CO;2-Y.

[36]T. Dumitrica, C. M. Landis and B. I. Yakobson, Curvature-induced polarization in carbon nanoshells, *Chem. Phys. Lett.* **360**, 182 (2002), https://doi.org/10.1016/S0009-2614(02)00820-5.
[37]S. I. Kundalwal, S. A. Meguid and G. J. Weng, Strain gradient polarization in graphene, *Carbon* **117**, 462 (2017), https://doi.org/10.1016/j.carbon.2017.03.013.
[38]Y. Gao and Z. L. Wang, Electrostatic potential in a bent piezoelectric nanowire. The fundamental theory of nanogenerator and nanopiezotronics, *Nano Lett.* **7**, 2499 (2007), https://doi.org/10.1021/nl071310j.